Translational Oncology
www.transonc.com
Volume 4 Number 3 June 2011 pp. 138–146 138

Bioengineered Human Arginase I with Enhanced Activity and Stability Controls Hepatocellular and Pancreatic Carcinoma Xenografts[1]

Evan S. Glazer*, Everett M. Stone†, Cihui Zhu*, Katherine L. Massey*, Amir N. Hamir‡ and Steven A. Curley*,§

*Department of Surgical Oncology, The University of Texas MD Anderson Cancer Center, Houston, TX, USA; †Department of Chemical Engineering, University of Texas at Austin, Austin, TX, USA; ‡Department of Veterinary Medicine and Surgery, The University of Texas MD Anderson Cancer Center, Houston, TX, USA; §Department of Mechanical Engineering and Materials Science, Rice University, Houston, TX, USA

Abstract

Hepatocellular carcinoma (HCC) and pancreatic carcinoma (PC) cells often have inherent urea cycle defects rendering them auxotrophic for the amino acid L-arginine (L-arg). Most HCC and PC require extracellular sources of L-arg and undergo cell cycle arrest and apoptosis when L-arg is restricted. Systemic, enzyme-mediated depletion of L-arg has been investigated in mouse models and human trials. Non–human enzymes elicit neutralizing antibodies, whereas human arginases display poor pharmacological properties in serum. Co^{2+} substitution of the Mn^{2+} metal cofactor in human arginase I (Co-hArgI) was shown to confer more than 10-fold higher catalytic activity (k_{cat}/K_m) and 5-fold greater stability. We hypothesized that the Co-hArgI enzyme would decrease tumor burden by systemic elimination of L-arg in a murine model. Co-hArgI was conjugated to 5-kDa PEG (Co-hArgI–PEG) to enhance circulation persistence. It was used as monotherapy for HCC and PC *in vitro* and *in vivo* murine xenografts. The mechanism of cell death was also investigated. Weekly treatment of 8 mg/kg Co-hArgI–PEG effectively controlled human HepG2 (HCC) and Panc-1 (PC) tumor xenografts ($P = .001$ and $P = .03$, respectively). Both cell lines underwent apoptosis *in vitro* with significant increased expression of activated caspase-3 ($P < .001$). Furthermore, there was evidence of autophagy *in vitro* and *in vivo*. We have demonstrated that Co-hArgI–PEG is effective at controlling two types of L-arg–dependent carcinomas. Being a nonessential amino acid, arginine deprivation therapy through Co-hArgI–PEG holds promise as a new therapy in the treatment of HCC and PC.

Translational Oncology (2011) 4, 138–146

Introduction

Hepatocellular carcinoma (HCC) and pancreatic carcinoma (PC) are two cancers that often depend on extracellular sources of the amino acid L-arginine (L-arg) for survival and experience cell cycle arrest and apoptosis in its absence [1–3]. Systemic depletion of circulating free L-arg has been used in multiple clinical trials [2]. The native human enzyme L-arginase I (hArgI), which uses two divalent manganese cations as an essential cofactor, is minimally active under physiological conditions (i) because it exhibits a low catalytic activity because of a very low saturation constant K_m (=2.3 mM) at the physiological pH of 7.4 and (ii) because, in serum, the Mn^{2+} ions are rapidly released from the protein, resulting in inactivation of the enzyme with a half-life of only 4.8 hours [4,5].

Non–human enzymes, such as arginine deiminase from *Mycoplasma arginini*, display increased activity and stability under physiological

Address all correspondence to: Steven A. Curley, MD, 1400 Holcombe Blvd, Unit 444, Houston, TX 77030. E-mail: scurley@mdanderson.org

[1]This work was funded by the National Institutes of Health (SAC, R01 CA139059) and by a grant from the Welch Foundation via TI-3D (E.M.S.). E.S.G. is a National Institutes of Health T32 research fellow (T32 CA09599). This research is supported in part by the National Institutes of Health through MD Anderson's Cancer Center Support grant CA016672. E.M.S. is listed as a co-inventor on a patent application on the Co-hArgI enzyme. The other authors declare no conflicts of interest.
Received 5 November 2010; Revised 5 November 2010; Accepted 4 January 2011

1944-7124/11
DOI 10.1593/tlo.10265

conditions and have been under clinical evaluation for HCC, metastatic melanoma, and small cell lung carcinoma (clinicaltrials.gov identifier: NCT01266018) [6–9]. In clinical practice, the immunogenicity induced by non–human proteins limits the effectiveness of these enzymes. Specifically, blocking antibodies limits the effectiveness of non–human enzymes. Pharmacologic immunosuppression is a theoretical option, but it is clearly inviting multiple further problems without a clear benefit.

Whereas patients with resectable HCC and PC have improved survival after resection, this is an option to very few patients and still does not offer a permanent cure in most instances. For those patients with unresectable HCC, sorafenib has been shown to improve overall survival rates by approximately 3 months [10]. Sorafenib constitutes the first targeted therapy for HCC that has proven effective, albeit with significant limitations and costs. Despite overexpression of numerous antigens, PC does not have any approved targeted therapies that significantly prolong survival, despite many therapies in clinical trials [11]. It has been suggested that the reason for this is that the extracellular stromal environment prevents targeted therapy from reaching the cancer cells and creates a promalignant environment [12,13]. Systemic depletion of circulating L-arg should bypass this phenomenon by equilibrating L-arg gradients away from the tumor directed out of the stromal microenvironment to the circulatory system for further degradation.

The native form of hArgI has been used in small trials with short-term success only [4]. Although there is some control of disease, most patients quickly progress without a durable benefit. The rationale for this is that the activity under physiological conditions (i.e., intravascular *in vivo*) is very low, with rapid inactivation. However, a cobalt-substituted hArgI has been demonstrated to be over 10-fold more active than native hArgI in physiologic conditions and is much more stable with a prolonged circulating half-life [5,14].

We hypothesized that HCC and PC xenografts would be susceptible, and there would be an antitumor response to systemic L-arg deprivation with a cobalt-substituted hArgI in a murine model.

Materials and Methods

Tumor Cell Lines, Murine Models, and Histology

The HCC cell line, HepG2, and the PC cell line, Panc-1, were acquired from the American Type Culture Collection (Manassas, VA) and kept in Dulbecco modified Eagle medium with 10% fetal bovine serum and 1% penicillin/streptomycin at standard conditions. L-Arg free Dulbecco modified Eagle medium was acquired from MP Biomedicals, LLC (Solon, OH). Cell lines were characterized by the Cell Line Characterization Core (MD Anderson Cancer Center, Houston, TX). For the *in vivo* experiments, 3×10^6 cells were injected in the right flank of nude BALB/c mice ($n = 10$ each cell line; NCI Mouse Repository, Frederick, MD). Treatment began when the tumors were palpable (approximately 4 weeks after injection) and occurred weekly after size measurements with a digital caliper (starting with week labeled "1" and volume = width^2 × length). Mice in two cages were combined and randomly chosen for the treatment groups. Within each cell line, controls were treated with equivolume phosphate-buffered saline by intraperitoneal (IP) injection, whereas the treatment groups received 8 mg/kg Co-hArgI IP. All mice were allowed standard rodent chow and water throughout the experiment *ad libitum*. The chow contained approximately 25% protein by volume and less than 1% L-arg.

A body condition score (BCS) assessed the health of the mice [15], and complete necropsy was performed to evaluate the evidence of treatment-related toxicity and tumor response. Specimens were prepared for histologic procedures by embedding in paraffin and sectioning at 5 μm. The sections were stained with hematoxylin and eosin and were examined by light microscopy. Injury to normal tissues was assessed by grade (grade 1: rare, <10%; grade 2: mild, 10%-20%; grade 3: moderate, 20%-50%; grade 4: severe, >50%) by an expert in mammalian pathology (A.N.H.).

PEGylation of Human Co-hArgI

Co^{2+}-substituted human hArgI was expressed in *Escherichia coli*, and the protein was purified as described previously [5] with the following exceptions: after binding to the immobilized metal affinity (IMAC) column, the protein was washed extensively (80-90 column volumes) with an IMAC buffer containing 0.1% Triton 114 to remove endotoxin and the buffer was exchanged into 100 mM $NaPO_4$ buffer, pH 8.3 using a 10,000 molecular weight cut off filtration device (Millipore Corp, Billerica, MA). Using a small reaction jar, Methoxy PEG Succinimidyl Carboxymethyl Ester 5000 MW (PEG-5K; JenKem Technology, Allen, TX) was added to Co-hArgI at a 40:1 molar ratio and allowed to react for 1 hour at 25°C under constant stirring. $CoCl_2$ was added to a final concentration of 10 mM, mixed, and heated at 50°C for 10 minutes. After centrifugation to remove any precipitates, the PEG-5K Co-hArgI was extensively buffer exchanged (phosphate-buffered saline [PBS] with 10% glycerol) using a 100,000 MWCO filtration device (Millipore Corp), sterilized by filtration through a 0.2-μm syringe filter (VWR, West Chester, PA), flash-frozen in liquid nitrogen, and stored at −80°C.

Mitochondrial Reductase Activity Analysis

HepG2 and Panc-1 cells were plated in 96-well plates at a density of 500 cells/well. Twenty-four hours later, groups of cells ($n = 8$) were treated with varying amounts of Co-hArgI or PBS. On days 1, 3, 5, and 7 after treatment, 100 μl of 3-(4,5-dimethyl-2-thiazolyl)-2,5-diphenyl-2*H*-tetrazolium bromide (MTT) was added to each well. Four hours later, the supernatant was aspirated, and 200 μl of DMSO was added to each well. Absorbance ca. 570 nm was measured (Synergy HT; BioTeck Instruments, Inc, Winooski, VT), corrected for blank DMSO, averaged for each group, and normalized to the absorbance value of PBS controls measured at the same time. Error bars are SEM. The 50% inhibitory concentration (IC_{50}) was determined by the Hill-Slope model [16].

Intracellular Protein Expression Measured with Immunoblot

In separate experiments, Panc-1 and HepG2 cells were treated with Co-hArgI at a final concentration of 1 nM or with an equal volume of PBS control. On days 1 and 4 after treatment, cell lysates were obtained with cold radioimmunoprecipitation assay buffer, incubated on ice for 30 minutes, and centrifuged at 13,000 rpm for 30 minutes. Proteins were resolved by SDS-PAGE on a Bis-Tris protein gel and transferred to a polyvinylidene fluoride membrane for Western blot analysis. The membranes were incubated in 5% nonfat dry milk for 1 hour and incubated with primary antibodies (BD Biosciences, Franklin Lakes, NJ; or Santa Cruz Biotechnology, Inc, Santa Cruz, CA). Next, the membranes were incubated with peroxidase-IgG at the dilution suggested by the manufacturer (H + L chains; Jackson Immuno Research Laboratories, West Grove, PA) and developed using the peroxidase substrate solution (GenDEPOT, Inc,

Barker, TX). Band intensity was determined using a high-resolution photo scanner (CanoScan 4400F; Canon, Inc, Lake Success, NY).

Flow Cytometric Analysis

Panc-1 cells or HepG2 cells were treated with Co-hArgI (1 nM final concentration in fresh complete media) or PBS (equivolume in fresh complete media) 24 hours after plating. Four days later, the cells were harvested after treatment with trypsin-EDTA (Mediatech, Inc, Manassas, VA). Next, the cells were washed with PBS followed by washing with Annexin buffer 1× (BD Biosciences). The cells were suspended in 100 μl of buffer and stained with 7-aminoactinomycin D (7-AAD; BD Biosciences) a fluorophore that binds to DNA in necrotic cells. Cells were also stained with Annexin V conjugated to Horizon V450 (BD Biosciences) to measure external phosphatidylserine expression. The cells were then twice washed with buffer and fixed/permeabilized with a paraformaldehyde-based kit (CytoPerm/CytoFix; BD Biosciences).

After permeabilization, intracellular staining was performed with fluorophore-labeled monoclonal antibodies according to the manufacturers' recommendations. A phycoerythrin-labeled antibody against the nuclear proliferation antigen Ki-67 (BD Biosciences), a fluorescein isothiocyanate–labeled antibody against activated caspase-3 (Santa Cruz Biotechnology, Inc), and a monoclonal antibody against urea cycle enzyme argininosuccinate synthetase-1 (ASS-1) conjugated to APC-H7 (provided as a kind gift from BD Biosciences) were added to each sample. The cells were gently mixed and then kept in the dark for 15 minutes at 4°C.

After staining, the cells were washed and suspended in ~200 μl of permeabilization buffer. Typically, for each sample 20,000 cells were analyzed by flow cytometry (LSRII Flow Cytometer; BD Biosciences), and the data were analyzed with FlowJo version 8.8.6 (TreeStar, Inc, Ashland, OR).

Activated Caspase-3 Expression in Ex Vivo *Tumor Sections*

Tumor sections on standard glass slides were deparaffinized by thrice passing into xylene and were subsequently rehydrated by a serial incubation in ethanol-water solutions with decreasing ethanol concentration. Next, the slides were washed and steamed in citrate buffer for 25 minutes, placed in methanol-hydrogen peroxide for 15 minutes, rinsed, and washed with PBS. Next, the sections were

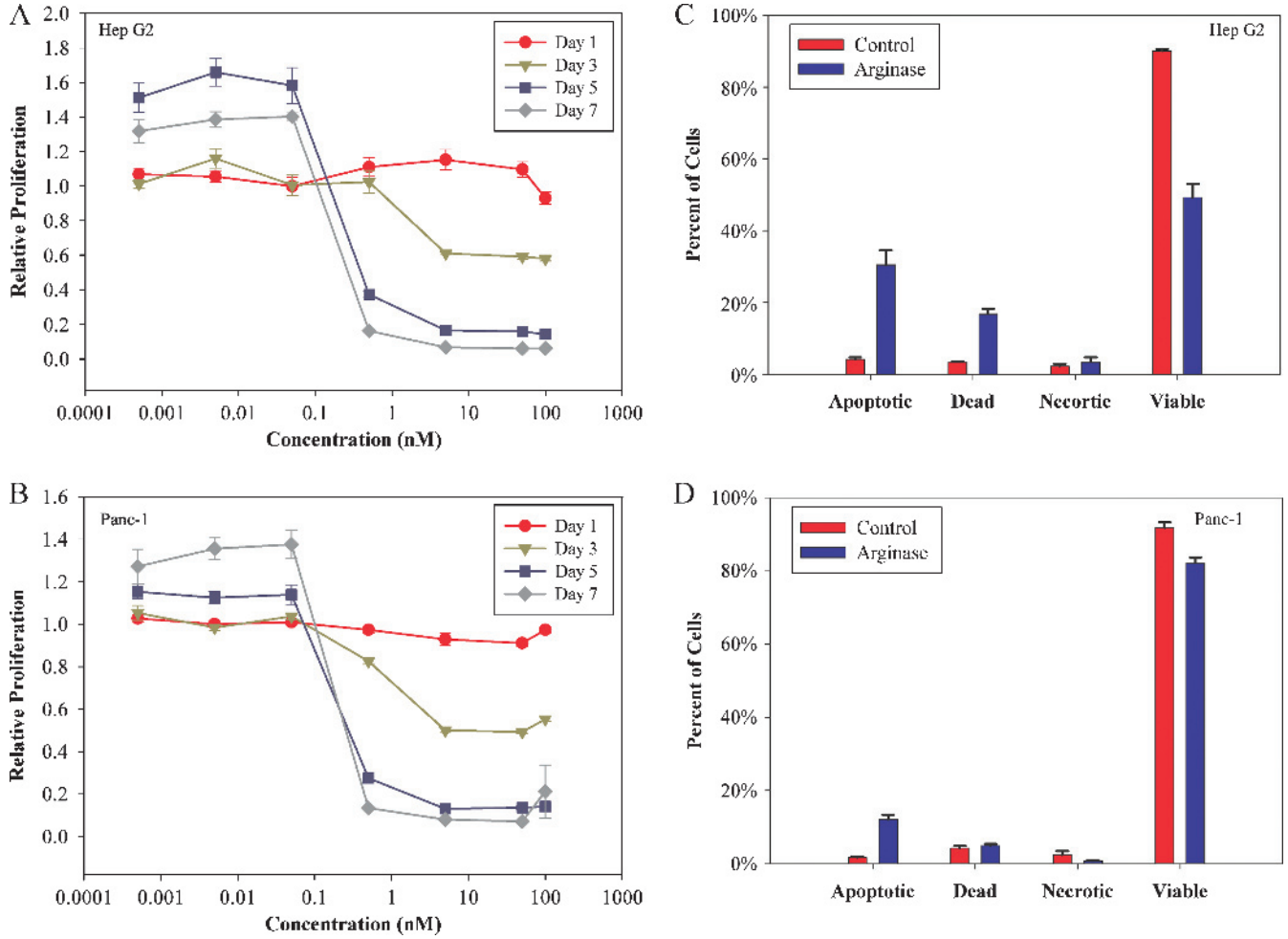

Figure 1. After day 1, the IC_{50} was 0.75 ± 0.36 and 0.44 ± 0.04 nM for HepG2 (A) and Panc-1 (B) cells, respectively, based on mitochondrial reductase activity (MTT). Flow cytometry demonstrated that HepG2 cells treated with 1 nM arginase (C) increased the apoptotic fraction (Annexin V–positive only, $P = .001$) and dead cell fraction (double positive for Annexin V and 7-AAD, $P = .0003$) with an appropriate decrease in viability (double negative, $P = .0001$). A similar decrease in the viability of Panc-1 cells was found (D), albeit less so when compared with the HepG2 cells ($P = .004$). Necrotic cells were identified as being Annexin V–negative, 7-AAD–positive cellular events.

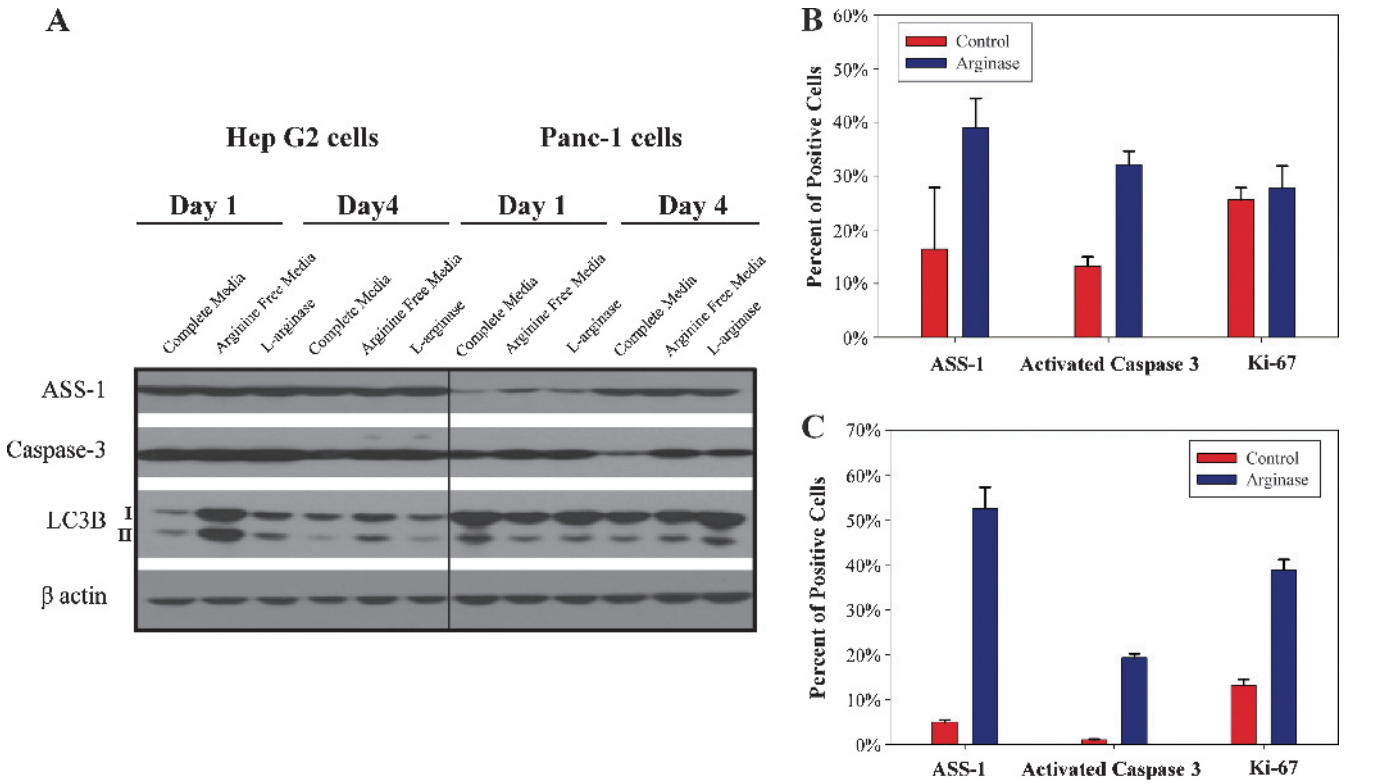

Figure 2. Protein immunoblot demonstrated increased levels of LC3B-II after a single day of treatment with 1 nM Co-hArgI or placement in L-arg–free medium in HepG2 cells (A). This continued but decreased by day 4 after treatment without medium replacement. Panc-1 cells initially had decreased levels of LC3B-II 1 day after treatment but increased expression by day 4. Activated (cleaved large fragment) caspase-3 increased slightly after 1 day of treatment in HepG2 cells, whereas this was more clearly seen for Panc-1 cells 4 days after treatment. Investigation with flow cytometry demonstrated that more individual Panc-1 cells (B) contained similar levels of ASS-1 (P = .13), increased levels of activated caspase-3 (P = .0009), and similar Ki-67 expression (P = .66) 4 days after L-arg treatment compared with control cells. Likewise, more HepG2 cells (C) expressed ASS-1 (P = .0001), activated caspase-3 (P < .0001), and Ki-67 (P = .0002). All media contained 10% FBS which may contain some L-arg.

blocked with 10% solution of Tween 20 with animal serum in PBS for 30 minutes. Anti–activated caspase-3 (cleaved large fragment) primary antibody at 1:250 dilution (Cell Signaling Technology, Inc, Danvers, MA) was added for 2 hours at 37°C in humidified air. Sections were washed with PBS, the secondary antibody was added for 30 minutes, washed, and DAB solution was applied according to the manufacturer's instructions (Vector Laboratories, Burlingame, CA). The sections were washed and counterstained with Mayer hematoxylin. After the final washing, the sections were sealed.

Confocal Microscopy of Ex Vivo *Tumor Sections*

After tumor sections were deparaffinized and rehydrated as above, slides were placed in boiling citrate antigen retrieval (freshly prepared 10 mM citric acid, 0.05% Tween 20, pH 6.0) for 15 minutes and blocked with 1% bovine serum albumin and 2% fetal bovine serum in PBS for 1 hour at room temperature. Primary antibodies for LC3B-II (1:250; Cell Signaling Technology, Inc) were diluted in blocking solution, and sections were covered for 1.5 hours at room temperature. The sections were thrice washed with PBS and covered with the secondary antibody conjugated to Alexa Fluor 488 (1:500 dilution) for 1 hour in the dark at room temperature (Cell Signaling Technology, Inc). Sections were then thrice washed with PBS and stained with 300 nM DAPI for 8 minutes (Invitrogen Corp, Carlsbad, CA). Finally, sections were washed in PBS and mounted in aqueous mounting medium (Dako North America, Inc., Carpinteria, CA) and sealed.

Statistics

Results are reported as mean ± SEM unless otherwise noted. Statistical significance, α, was set to P = .05. Two-tailed Student's t test compared differences in means between groups, whereas multiway analysis of variation analyzed tumor volumes (SPSS version 16.0; SPSS, Inc, Chicago, IL). Data were plotted with Sigma Plot Version 11 (Systat Software, Inc, San Jose, CA).

Results

Co-hArgI Treatment Induces Cell Death of HepG2 and Panc-1 Cancer Cell Lines

As shown in Figure 1, both the HCC cell line HepG2 and the PC cell line Panc-1 demonstrated a concentration-dependent sensitivity to treatment with Co-hArgI as determined from the decrease in mitochondrial reductase activity (MTT). Panc-1 cells were slightly more sensitive than HepG2 cells to exposure of Co-hArgI (Figure 1), with IC_{50} values of 0.75 ± 0.36 and 0.44 ± 0.04 nM for HepG2 and Panc-1 cells, respectively. At concentrations less than 0.1 nM, both cell lines had adequate nutrition to proliferate 5 to 7 days after treatment compared with PBS controls on the first day. Detection of

Annexin V levels and 7-ADD staining indicated that HepG2 cells and Panc-1 cells displayed increased rates of apoptotic cell death 4 days after treatment with 1 nM Co-hArgI (Figure 1).

There was a slight increase in activated cleaved caspase-3 in HepG2 and Panc-1 cells after a single day of Co-hArgI treatment based on immunoblot (Figure 2*A*). Whereas HepG2 cells expressed increased amounts of LC3B-II (a marker of autophagy) after a single day of treatments, it was not as much as the positive control (L-arg–free media; Figure 2*A*). Interestingly, Panc-1 cells did not demonstrate early increased expression of LC3B-II 1 day after treatment, whereas it was seen 4 days after treatment (Figure 2*A*). On the basis of protein immunoblot, Panc-1 cells increased the total expression of the rate-limiting enzyme in endogenous L-arg production, ASS-1 (Figure 2*A*), whereas HepG2 cells show no appreciable difference (Figure 2*A*) both as a function of time and treatment.

In addition to protein immunoblots that measure proteins in a population of cells, we used flow cytometry to analyze the difference between PBS-treated control cells and 1-nM Co-hArgI–treated cells as a percent of the population overexpressing a given protein at the single-cell level not the total protein expression in a sample (Figure 2, *B* and *C*). There were significantly more cells with increased levels of ASS-1 protein production after Co-hArgI treatment in the HepG2 cell line ($P = .0001$) but not in the Panc-1 cell line ($P = .13$). Activated caspase-3 was increased significantly for both cell lines ($P < .0001$ for HepG2 and $P = .0009$ for Panc-1 cells). Interestingly, the proportion of cells expressing Ki-67 did not change for Panc-1 cells (Figure 2*B*, $P = .66$), whereas the proportion of HepG2 cells expressing elevated levels of Ki-67 nearly tripled after Co-hArgI treatment (Figure 2*C*; $P = .0002$).

Destruction of Established HepG2 and Panc-1 Tumor Xenografts

Weekly treatment with PEG-Co-hArgI at 8 mg/kg began after week 1 (Figure 3). Although there was no response after 1 week of treatment, by week 3, Panc-1 tumors from treated mice grew more slowly than tumors from control mice (Figure 3*A*; overall $P = .03$). However, soon after treatment began in mice with HepG2 tumors, differences in tumor volumes could be seen and continued for the duration of the experiment (Figure 3*B*; overall $P = .001$). Of the HepG2 tumors, two-fifths demonstrated nearly complete response to arginase treatment (Figure 3*C*). Representative sections of HepG2 tumors are shown demonstrating increased grades of necrosis (control [Figure 4*A*] compared to treatment [Figure 4*B*]), increased amounts of cleaved caspase-3 (control [Figure 4*C*] compared to treatment [Figure 4*D*]), and increased presence of autophagosomes as measured by LC3B-II (control [Figure 4*E*] compared to treatment [Figure 4*F*]) that were seen in the tumors. Furthermore, regions of tumor from the PBS-treated mice (Figure 4*A*) demonstrate larger and presumably healthier vasculature (*bright red*) not seen in the tumors from Co-hArgI–treated mice (Figure 4*B*).

Toxicity Associated with Arginase Treatment

Mice treated with greater than 15-mg/kg Co-hArgI demonstrated significant toxicity (weight loss, hunch posture, lethargy) requiring euthanasia in accordance with the humane treatment of animals. Full necropsies were performed, and the only evidence of histologic abnormality was bone marrow devastation in a concentration-dependent manner (Figure 5*A*). Low-dose Co-hArgI (<10 mg/kg) and control mice did not demonstrate bone marrow injury (Figure 5*B*). Weight loss, as well, was dependent on the dose of arginase received (Figure 5*C*). No other major organ such as brain, heart, lung, kidney, liver, or gastrointestinal tract demonstrated any insults on gross examination or histologic evaluation.

Discussion

We have demonstrated that Co-hArgI affects the growth of human HCC and PC xenografts in a murine model. The rationale for systemic arginine deprivation therapy for HCC or PC is not a new idea, but the difficulty has been doing so in an effective and nonimmunogenic

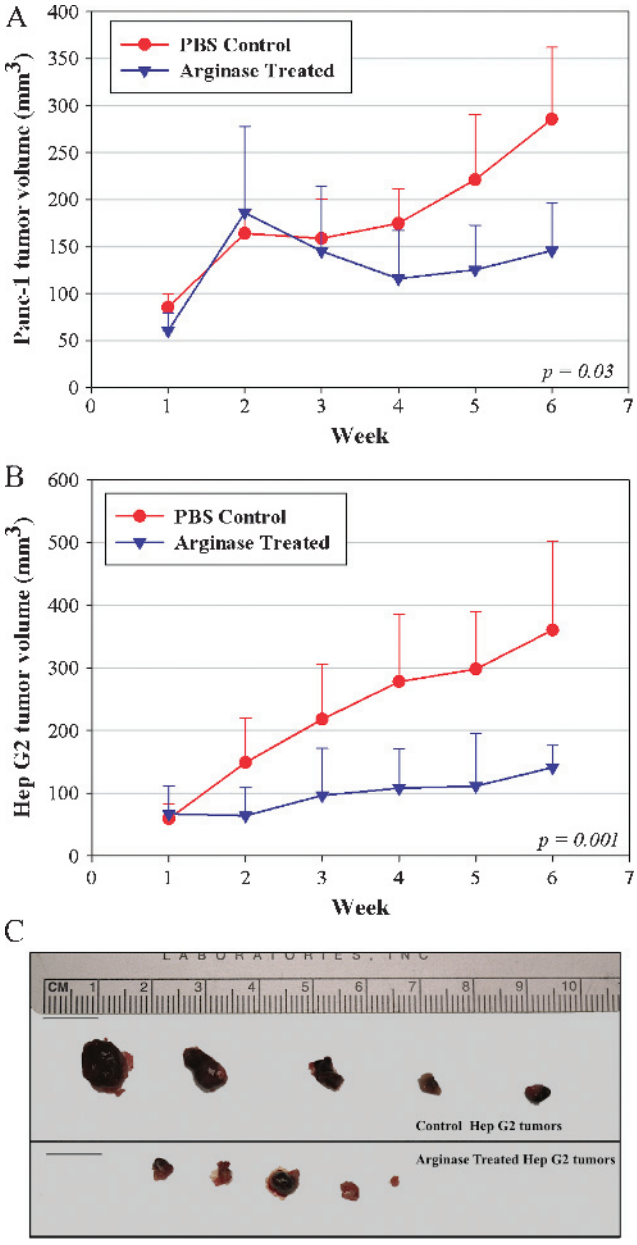

Figure 3. (A) Panc-1 subcutaneous xenografts in nude BALB/c mice demonstrated decreased tumor volume due to treatment with 8 mg/kg Co-hArgI–PEG ($P = .03$). (B) Likewise, HepG2 subcutaneous xenografts also demonstrated significantly smaller tumors, but they did so within 1 week of treatment ($P = .001$). (C) At the end of the experiment, PEG–Co-hArgI–treated tumors were much smaller as exemplified in the HepG2 tumors.

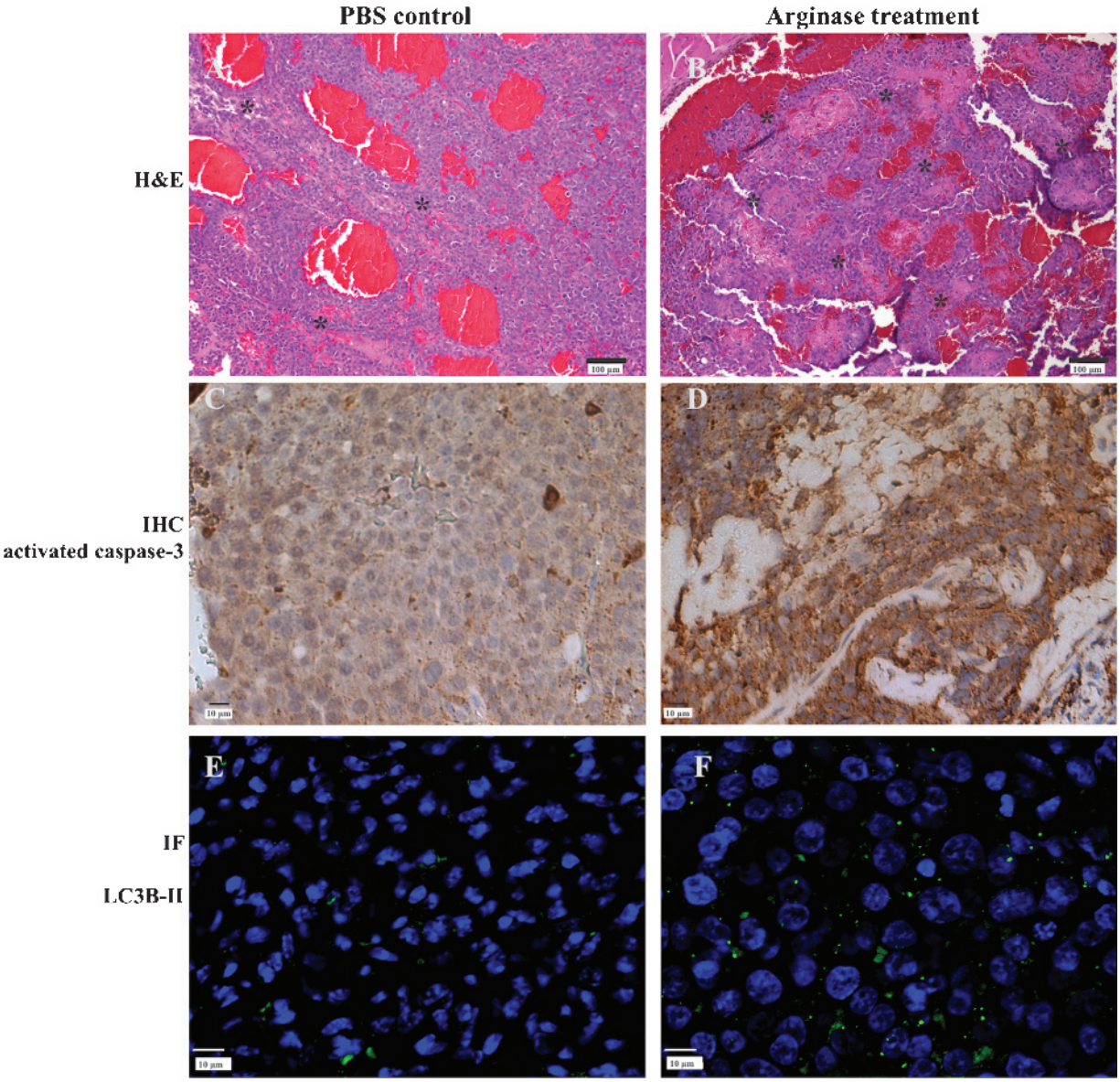

Figure 4. Although there is some necrosis (*) in HepG2 tumors from mice treated with PBS controls (A; hematoxylin and eosin stain, bright red areas are intravascular blood), there was significantly higher grades of necrosis in the tumors from arginase-treated mice (B). Likewise, a few cells in control tumors expressed activated caspase-3 (C; immunohistochemistry [IHC]), although significantly more cells expressed activated caspase-3 after Co-hArgI treatment (D). Finally, tumors from control-treated mice demonstrated far fewer autophagosomes (E; immunofluorescence [IF]; green label is LC3B-II, whereas blue label is DAPI) than tumors from arginase-treated mice (F). Larger nuclei (blue) are seen with Co-hArgI treatment (D, F).

manner [7,17]. Other therapies have failed because they use foreign proteins inducing an immunogenic response, or they are enzymes that are minimally active in physiologic intravascular conditions. We have solved these problems by using a minimally engineered human enzyme with improved kinetics and stability that should eliminate or greatly reduce host immunogenic responses. Formal toxicity studies will be performed in the near future to verify this. Clearly, individual patient variations may limit the effectiveness of Co-hArgI, but we believe that starting with a stabilized human enzyme is promising. We estimate that the toxicity seen *in vivo* occurs at more than 200× the *in vitro* concentration used herein. It is inappropriate to assume that human toxicity data will be the same as mouse; however, these data are suggestive that there will be a reasonable therapeutic window for clinical trials.

Small case reports that demonstrate effectiveness of endogenous arginase reassure that the minimally engineered Co-hArgI should be effective at depleting systemic L-arg levels [18]. Furthermore, depleting systemic L-arg has resulted in decreased HCC tumor burdens in multiple human and animal studies with multiple other enzymes [4,7,18]. The principle of this therapy remains the same, but identifying the least toxic and least immunogenic modality has been the major challenge. The toxicity seen in mice herein and the duration to recovery (i.e., normalization of BCS scores) limited the treatment interval to weekly while permitting some L-arg reconstitution in the serum from dietary sources (data not shown). Clinical effectiveness will determine the appropriate balance of treatment dose, interval, and adverse events.

The differences in mitochondrial activity (MTT assay), decrease in viability (as defined by Annexin V and propidium iodide double

positivity), and caspase-3 expression demonstrate some variability in cellular death at the single-cell resolution (Figures 1 and 2). We theorize that this is due to the balance of availability of L-arg and cellular responses to maintain homeostasis (i.e., autophagy seen in the L-arg–free media). In addition, cells that are more sensitive to L-arg deprivation respond sooner, whereas cells able to maintain homeostasis do not respond as quickly.

The observed slight induction of cleaved caspase-3 and increased presence of autophagosomes are not unexpected. Discrepancies between the immunoblot and flow cytometric data suggest that subpopulations of cells exist that respond differently at the individual cell level. Both activated/cleaved caspase-3 and autophagosome productions have been previously demonstrated during amino acid deprivation therapy, in general, and L-arg deprivation specifically [9,14,19]. Interestingly, other groups have investigated a caspase-independent pathway toward cell death via autophagy in prostate cancer xenografts treated with L-arg deprivation therapy [20]. This supports studies suggesting a role for selective autophagy in cancer development [21]. An inadequate supply of circulating L-arg coupled with an inability to synthesize more may increase genomic instability and aberrant signaling pathways [21]. The results here neither confirm nor contradict this finding because we did not investigate these pathways as deeply as the other studies. However, it is interesting that we found evidence of both cleaved caspase-3 and autophagosomes *in vitro* and *in vivo*. HepG2 cells demonstrated increased levels of LC3B-II more so than Panc-1 cells (Figure 2*A*). This suggests that various cancers may succumb to treatment through different pathways, something under active research. Simultaneously, Panc-1 cells demonstrated relatively more activated caspase-3 than HepG2 cells 4 days after treatment (Figure 2*A*). It is likely that bioengineered Co-hArgI will be useful as part of a multimodal therapy for HCC or PC. This is especially true as new therapies develop based on the modulation of multiple pathways (i.e., caspase cascade or autophagy), where the combination may be effective in treating many types of susceptible solid organ malignancies.

The increase in Ki-67 expression *in vitro* and increased nuclear size *in vivo* is very interesting. In humans, multiple studies have demonstrated correlations between nuclear size (morphometry) and increased Ki-67 expression in solid organ malignancies similar to those demonstrated here (Figures 2*C* and 4*F*) [22–25]. We expected that cellular processes would decrease during L-arg deprivation and result in decreased Ki-67. However, we theorize that continued proliferation despite decreased L-arg reserves is characteristic of L-arg auxotrophy in this model. The total cellular mass is decreased based on MTT data *in vitro* and reduced tumor sizes *in vivo*. Therefore, we believe that HepG2 cells continue active metabolic pathways in the attempt to acquire more L-arg through autophagy but cannot do so and eventually die. This somewhat unexpected correlation between Ki-67 expression and autophagy has been demonstrated in human gastrointestinal cancers [26], as has the correlation between activated/cleaved caspase-3 and LC3B-II expression [27]. Panc-1 cells, however, do not increase their intrinsic metabolic rates and hence are able to live longer (and hence, tumors remain larger), whereas mitochondrial reductase activity remains low overall. This is consistent with a G_0/G_1 block that we have previously demonstrated [14].

It seems from ASS-1 expression levels that at least some Panc-1 and HepG2 cells are attempting to replenish L-arg levels. However, this occurs several enzymatic steps upstream of ASS-1–mediated synthesis of argininosuccinate from L-citrulline, aspartate, and ATP. HepG2 cells (and other HCC models) have previously demonstrated to be particularly sensitive to L-arg depletion with arginase treatment as opposed to arginine deiminase treatment because those cells cannot consistently and simultaneously produce sufficient amounts of both ASS-1 and ornithine transcarbamylase for L-arg production [1,3,28]. Thus far, L-arg auxotrophy in some pancreatic tumors seems to be primarily a function of ASS-1 down-regulation, so it is

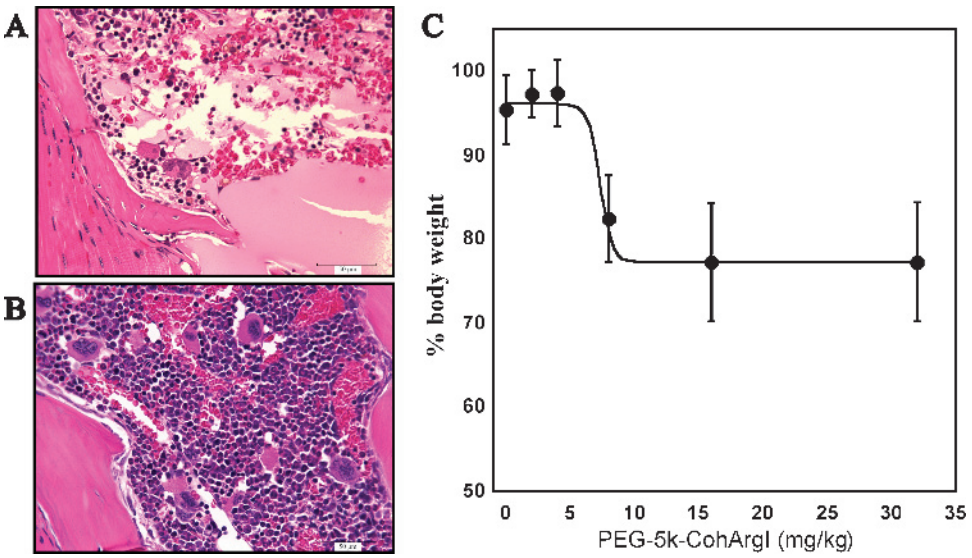

Figure 5. Arginase-related toxicity was found in mice treated at doses of 15 mg/kg or greater. On necropsy, the only evidence of normal tissue toxicity was massive bone marrow devastation (A), whereas control bone marrow remained normal (B). In addition, weight loss was measured as a function of dose-dependent toxicity (0-32 mg/kg, $n = 5$ each) after IP injection of L-arg. The greatest observed weight loss occurred 4 days after treatment (C). The 16- and 32-mg/kg groups had a BCS of 1 and were killed for humane reasons. The mice in the 8-mg/kg group had a BCS score of 2 to 3 and regained their original body mass in an additional 2 to 3 days.

interesting that unlike previous reports, we were able to observe some ASS-1 protein in Panc-1 cells [1]. Furthermore, we describe that, for our control Panc-1 cells, depletion of all arginine in the medium results in increased ASS-1 production over time not seen in HepG2 cells. The discrepancy between previous reports and data herein may relate to the degree of insult induced by the arginine deprivation therapy. Finally, the level of ASS-1 production may determine how subpopulations of cells respond in terms of apoptosis, autophagy, and/or cell death.

In vitro, the potent IC_{50} values of Co-hArgI toward both HepG2 and Panc-1 cells are similar, suggesting that the urea cycle is not sufficiently intact in either tumor type to produce enough L-arg internally for continued growth in the face of extrinsic arginine depletion. We theorize that the discrepancy between population immunoblot measurements of ASS-1 and individual cell flow cytometric measurements suggests that there are variations in cell subpopulations. Likely, nonspecific amino acid transporters allow for L-arg to be "shared" in the cell cultures, decreasing the need for ASS-1 in some cell subpopulations.

In vivo, however, Co-hArgI–PEG shows a more robust response toward HepG2 than Panc-1. It is likely that the slower metabolism of Panc-1 cells in the *in vivo* mouse xenograft model allows them to withstand the periods of L-arg depletion longer than the more metabolically active HepG2 cells. However, modulation in Co-hArgI–PEG dosing in mice may allow longer L-arg depletion times, but this is precluded by toxic bone marrow suppression effects at very high doses of Co-hArgI–PEG in mice with unclear consequences in humans. We suspect that the more resilient Panc-1 tumors will require longer L-arg depletion times than can be safely withstood in mice. In humans, however, long-term L-arg depletion by arginine deaminase has been well tolerated, with the exception that neutralizing antibodies eventually develop [7], thus diminishing the effectiveness of this mycoplasmic enzyme in the long term.

A major drawback to this study is that only two cell lines were investigated. We chose to investigate two specific cancers that have very few effective therapies. Multiple studies from *in vitro* analyses to phase 2 clinical trials have demonstrated that arginine deprivation therapy is effective, albeit for short-term treatments only. However, we sought to investigate the use of a novel, bioengineered human enzyme. The fact that it was effective at safe concentrations *in vivo* suggests that further studies are warranted, although we only used two cell lines. In addition, further investigation requires determining whether autophagy or apoptosis is the primary means of cell demise. Likewise, investigations regarding these complex-signaling pathways are needed. Whereas there is evidence in the literature of both processes, and evidence herein to the same, much still needs to be elucidated as to which is most important and methods to combine treatments for maximum cancer therapy.

In summary, we have demonstrated the first *in vivo* data regarding a highly active, cobalt-substituted human arginase for the treatment of HCC and PC. The therapy was well tolerated in two murine xenograft models, with promising results. Further studies are underway with HCC, PC, and other cancer models with plans for future clinical trials.

Acknowledgments

The authors thank Kristine Ash and Yolanda Brittain from the Department of Surgical Oncology, University of Texas MD Anderson Cancer Center, for administrative assistance. The authors also thank the staff and animal care technologists of the Department of Veterinary Medicine and Surgery, specifically Maurice J. Dufilho, IV, and Courtney D. Vallien. Jared K. Burks of the Flow Cytometry and Cellular Imaging Core, University of Texas MD Anderson Cancer Center (NCI Core Grant CA16672), provided invaluable assistance with confocal microscopy. The authors thank Robert Balderas and Li Liu from BD Biosciences for providing the ASS-1 fluorophore conjugate.

References

[1] Bowles TL, Kim R, Galante J, Parsons CM, Virudachalam S, Kung HJ, and Bold RJ (2008). Pancreatic cancer cell lines deficient in argininosuccinate synthetase are sensitive to arginine deprivation by arginine deiminase. *Int J Cancer* **123**, 1950–1955.

[2] Feun L, You M, Wu CJ, Kuo MT, Wangpaichitr M, Spector S, and Savaraj N (2008). Arginine deprivation as a targeted therapy for cancer. *Curr Pharm Des* **14**, 1049–1057.

[3] Dillon BJ, Prieto VG, Curley SA, Ensor CM, Holtsberg FW, Bomalaski JS, and Clark MA (2004). Incidence and distribution of argininosuccinate synthetase deficiency in human cancers: a method for identifying cancers sensitive to arginine deprivation. *Cancer* **100**, 826–833.

[4] Cheng PN, Lam TL, Lam WM, Tsui SM, Cheng AW, Lo WH, and Leung YC (2007). Pegylated recombinant human arginase (rhArg-peg5,000mw) inhibits the *in vitro* and *in vivo* proliferation of human hepatocellular carcinoma through arginine depletion. *Cancer Res* **67**, 309–317.

[5] Stone EM, Glazer ES, Chantranupong L, Cherukuri P, Breece RM, Tierney DL, Curley SA, Iverson BL, and Georgiou G (2010). Replacing Mn(2+) with Co(2+) in human arginase I enhances cytotoxicity toward L-arginine auxotrophic cancer cell lines. *ACS Chem Biol* **5**, 333–342.

[6] Delman KA, Brown TD, Thomas M, Ensor CM, Holtsberg FW, Bomalaski JS, Clark MA, and Curley SA (2005). Phase I/II trial of pegylated arginine deiminase (ADI-PEG20) in unresectable hepatocellular carcinoma. *J Clin Oncol* **23**, 4139.

[7] Glazer ES, Piccirillo M, Albino V, Di Giacomo R, Palaia R, Mastro AA, Beneduce G, Castello G, De Rosa V, Petrillo A, et al. (2010). Phase II study of pegylated arginine deiminase for nonresectable and metastatic hepatocellular carcinoma. *J Clin Oncol* **28**, 2220–2226.

[8] Izzo F, Marra P, Beneduce G, Castello G, Vallone P, De Rosa V, Cremona F, Ensor CM, Holtsberg FW, Bomalaski JS, et al. (2004). Pegylated arginine deiminase treatment of patients with unresectable hepatocellular carcinoma: results from phase I/II studies. *J Clin Oncol* **22**, 1815–1822.

[9] Savaraj N, You M, Wu C, Wangpaichitr M, Kuo MT, and Feun LG (2010). Arginine deprivation, autophagy, apoptosis (AAA) for the treatment of melanoma. *Curr Mol Med* **10**, 405–412.

[10] Llovet JM, Ricci S, Mazzaferro V, Hilgard P, Gane E, Blanc JF, de Oliveira AC, Santoro A, Raoul JL, Forner A, et al. (2008). Sorafenib in advanced hepatocellular carcinoma. *N Engl J Med* **359**, 378–390.

[11] Philip PA (2010). Novel targets for pancreatic cancer therapy. *Surg Oncol Clin N Am* **19**, 419–429.

[12] Hwang RF, Moore T, Arumugam T, Ramachandran V, Amos KD, Rivera A, Ji B, Evans DB, and Logsdon CD (2008). Cancer-associated stromal fibroblasts promote pancreatic tumor progression. *Cancer Res* **68**, 918–926.

[13] Teicher BA (2009). Acute and chronic *in vivo* therapeutic resistance. *Biochem Pharmacol* **77**, 1665–1673.

[14] Glazer ES, Kaluarachchi WD, Massey KL, Zhu C, and Curley SA (2010). Bioengineered arginase I increases caspase-3 expression of hepatocellular and pancreatic carcinoma cells despite induction of argininosuccinate synthetase-1. *Surgery* **148**, 310–318.

[15] Ullman-Cullere MH and Foltz CJ (1999). Body condition scoring: a rapid and accurate method for assessing health status in mice. *Lab Anim Sci* **49**, 319–323.

[16] *Assay Guidance Manual Version 5.0* (2008). Eli Lilly and Company and NIH Chemical Genomics Center. Available at: http://www.ncgc.nih.gov/guidance/manual_toc.html. Accessed May 1, 2010.

[17] Ni Y, Schwaneberg U, and Sun ZH (2008). Arginine deiminase, a potential anti-tumor drug. *Cancer Lett* **261**, 1–11.

[18] Cheng PN, Leung YC, Lo WH, Tsui SM, and Lam KC (2005). Remission of hepatocellular carcinoma with arginine depletion induced by systemic release of

endogenous hepatic arginase due to transhepatic arterial embolisation, augmented by high-dose insulin: arginase as a potential drug candidate for hepatocellular carcinoma. *Cancer Lett* **224**, 67–80.

[19] Kim RH, Bold RJ, and Kung HJ (2009). ADI, autophagy and apoptosis: metabolic stress as a therapeutic option for prostate cancer. *Autophagy* **5**, 567–568.

[20] Kim RH, Coates JM, Bowles TL, McNerney GP, Sutcliffe J, Jung JU, Gandour-Edwards R, Chuang FY, Bold RJ, and Kung HJ (2009). Arginine deiminase as a novel therapy for prostate cancer induces autophagy and caspase-independent apoptosis. *Cancer Res* **69**, 700–708.

[21] Dikic I, Johansen T, and Kirkin V (2010). Selective autophagy in cancer development and therapy. *Cancer Res* **70**, 3431–3434.

[22] Nakajima T, Nakashima T, Okada Y, Jo M, Nishikawa T, Mitsumoto Y, Katagishi T, Kimura H, Itoh Y, Kagawa K, et al. (2010). Nuclear size measurement is a simple method for the assessment of hepatocellular aging in non-alcoholic fatty liver disease: comparison with telomere-specific quantitative FISH and p21 immunohistochemistry. *Pathol Int* **60**, 175–183.

[23] Ozer E, Yorukoglu K, Mungan MU, Ozkal S, Demirel D, Sagol O, and Kirkali Z (2001). Prognostic significance of nuclear morphometry in superficial bladder cancer. *Anal Quant Cytol Histol* **23**, 251–256.

[24] Buhmeida A, Pyrhonen S, Laato M, and Collan Y (2006). Prognostic factors in prostate cancer. *Diagn Pathol* **1**, 4.

[25] Ikeguchi M, Oka S, Saito H, Kondo A, Tsujitani S, Maeta M, and Kaibara N (2000). Nuclear accumulation of p53 protein in gastric cancer strongly correlates with enlargement of nuclear area of cancer cells. *Oncol Rep* **7**, 579–584.

[26] Yoshioka A, Miyata H, Doki Y, Yamasaki M, Sohma I, Gotoh K, Takiguchi S, Fujiwara Y, Uchiyama Y, and Monden M (2008). LC3, an autophagosome marker, is highly expressed in gastrointestinal cancers. *Int J Oncol* **33**, 461–468.

[27] Lin HM, Tseng HC, Wang CJ, Chyau CC, Liao KK, Peng PL, and Chou FP (2007). Induction of autophagy and apoptosis by the extract of *Solanum nigrum* Linn in HepG2 cells. *J Agric Food Chem* **55**, 3620–3628.

[28] Miyazaki K, Takaku H, Umeda M, Fujita T, Huang WD, Kimura T, Yamashita J, and Horio T (1990). Potent growth inhibition of human tumor cells in culture by arginine deiminase purified from a culture medium of a *Mycoplasma*-infected cell line. *Cancer Res* **50**, 4522–4527.